Seasonal occurrence, source apportionment, and cancer risk assessment of PAHs in the second largest international holy metropolitan: Mashhad,

Mahdad, Faezeh ; Riyahi Bakhtiari, Alireza ; Moeinaddini, Mazaher ; Charlesworth, Sue.

DOI 10.1007/s11356-021-16336-6
ISSN 0944-1344
ESSN 1614-7499

Publisher: Springer

The final publication is available at Springer via https://doi.org/10.1007/s11356-021-16336-6

Seasonal occurrence, source apportionment, and cancer risk assessment of PAHs in the second largest international holy metropolitan: Mashhad, Iran

Faezeh Mahdad [a], Alireza Riyahi Bakhtiari [a *], Mazaher Moeinaddini [b], Susanne Charlesworth[c]

[a] Department of Environmental Sciences, Faculty of Natural Resources and Marine Sciences, Tarbiat Modares University, Noor, Mazandaran, Iran

[b] Department of Environmental Sciences, Faculty of Natural Resources, University of Tehran, Karaj, Iran

[C] Centre for Agroecology, Water and Resilience, Coventry University, Coventry, United Kingdom

Abstract

Street dust resuspension is one of the main sources of particulate matter with impacts on air quality, health and climate. This research was aimed to determine the concentration, source, and health risk of polycyclic aromatic hydrocarbons (PAHs) in street dust of Mashhad city. To this end, PAHs were measured in 84 dust samples using gas chromatography coupled to mass spectrometry (GC-MS). The source of PAHs was identified using diagnostic ratios (DRs), positive matrix factorization (PMF), and principal component analysis (PCA). The measured PAHs demonstrated different spatial concentrations (from 1,005 μg kg^{-1} to 9,138.96 μg kg^{-1}) and showed higher levels in summer (1,206.21-9,138.96 μg kg^{-1}), although 4-ring PAHs exhibited maximum levels in both summer and winter. The findings revealed that the dust-deposited PAHs are predominantly emitted through combustion of fossil fuels (such as diesel and gasoline) and natural gas. The total incremental lifetime cancer risk (ILCR) was assessed

by considering three possible exposure routes separately for children and adults, and revealed carcinogenic risk values of 2.24E-06 and 2.14E-06, respectively. for children and adults in both seasons, about two times higher than the baseline value (1.0E-06).

Keywords: street dust, PAHs, air pollution, source apportionment, health risk assessment.

Introduction

Street dust can be considered as an archive of various urban air pollutants and could represent air quality (Alves et al., 2019). The street dust in urban areas contains a heterogeneous mixture of particles mainly produced by anthropogenic causes, such as vehicle exhausts, brake wears, tire debris, building demolitions, construction materials, wear of road pavement material or asphalt, and lubricant oil spill (Pant and Harrison, 2013). Due to the small size of resuspended dust particles and their intrinsic mobility, both direct (such as inhalation and ingestion) and indirect (such as skin) exposure cause human health risks (Zhen et al., 2020). Therefore, it is of high importance to measure the concentration of pollutants in street dust, identify their sources, and assess the potential hazards (Alves et al., 2019).

Polycyclic aromatic hydrocarbons (PAHs) are one the most ubiquitous classes of persistent organic pollutants (POPs) mainly found in urban environments (Liu et al., 2019). Due to their severe toxicity and prevalence, 16 PAHs have been identified as high priority pollutants by the United States Environmental Protection Agency (USEPA) (Ali et al., 2020). These organic molecules have attracted serious attention because of their carcinogenic and mutagenic nature (Huo et al., 2019) as well as remarkable environmental persistence (Liu et al., 2019; Wang et al., 2017). In the urban environments, PAHs are predominately released through incomplete combustion of organic materials (e.g., liquid fossil fuel, crude oil, and gas) by vehicles and power plants and spill of petroleum-based products by industrial and waste treatment processes

(Dong and Lee, 2009). Moreover, atmospheric precipitation (rain, snow, fog), as well as aerosols and gases, is another source of PAHs in urban areas (Franco et al., 2017; Škrbić et al., 2019). Depending on the emitting sources, two categories of PAHs with two or more fused benzene rings arranged in various configurations are produced; molecules with 2-3 rings are mainly produced by petrogenic sources but the others by pyrogenic ones (Moeinaddini et al., 2014b).

PAHs can bound to street dust and other particulate matters because of their semi-volatile feature; that is, these organic molecules could accumulate in eventually harmful quantities. Surface dust resuspension by wind or vehicle motion and, in turn, exposure to the dust-bound PAHs could induce adverse human health risks, especially in metropolitans (Pant and Harrison, 2013; Škrbić et al., 2019). Previous research reported a wide variety of health risks caused by PAHs, including skin, lung, bladder, and gastrointestinal cancers, DNA damages, cataracts, kidney dysfunctions, and liver diseases (Kim et al., 2013). Hence, characterizing the origin and dominant sources as well as the distribution and concentration of PAHs in the street dust is of high importance to design appropriate risk assessments and management strategies (Garcia et al., 2014; Ghanavati et al., 2019; Moeinaddini et al., 2014a; Pant and Harrison, 2013; Teixeira et al., 2015; Wang et al., 2017). Source apportionment of PAHs is performed through different approaches. Source apportionment of PAHs is performed through different approaches (Aldabe et al., 2011; Javed et al., 2019; Teixeira et al., 2015; Teixeira et al., 2013; Zheng et al., 2017). One of the methods is the Positive Matrix Factorization (PMF) model that mathematically apportions the sources of PAHs based on the concentrations measured at the receptor site (Li et al., 2017; Teixeira et al., 2015; Teixeira et al., 2013; Zheng et al., 2017).

Mashhad is the largest and second largest religious city in Iran and the world, respectively. Concerning air quality, this metropolitan ranks the second polluted city in Iran because of its increasing constant population and industrial activity as well as attracting over 20 million

77 foreign tourists and pilgrims from Azerbaijan, Bahrain, Kuwait, Iraq, Lebanon, Pakistan,
78 Afghanistan, and Qatar which annually visit the city (Azari and Arintono, 2012; Talebian and
79 Riza, 2020). Despite the crucial national and international importance of Mashhad city, there
80 remains a paucity of evidence concerning the contamination of the USEPA's 16 priority PAHs
81 in the urban area. Therefore, the present research was aimed to quantitatively and qualitatively
82 assess the concentration of PAHs in street dust of Mashhad, analyze the spatio-temporal
83 variation and distribution of PAHs, identify the PAHs sources using DRs (diagnostic ratios),
84 PCA (principal component analysis), and PMF (positive matrix factorization), and determine
85 the human health risk of PAHs through the incremental lifetime cancer risk (ILCR) method.

86 **2. Material and methods**

87 **2.1. Study area and Sampling**

88 Mashhad city is located in the north-east of Iran (36° 21' 28" N; 59° 33' 20" E), about 985
89 m above sea level (Fig. 1). The area has a temperate climate and annually experiences 270-300
90 days of thermal inversion. Street dust was collected from 42 locations with five replicates in
91 September 2018 and January 2019 (Fig. 1). The sampling was performed in dry weather, and
92 the collected dust was kept in a solvent-wrapped aluminum foil bag and stored at −20 °C until
93 the laboratory analysis (Azimi et al., 2018; Najmeddin and Keshavarzi, 2019). The samples
94 were dried at room temperature using a desiccator and then passed through a stainless steel
95 sieve (63 μm mesh). The sieved dust samples were stored at −4 °C in a refrigerator for PAHs
96 analyses (Dong and Lee, 2009; Škrbić et al., 2019).

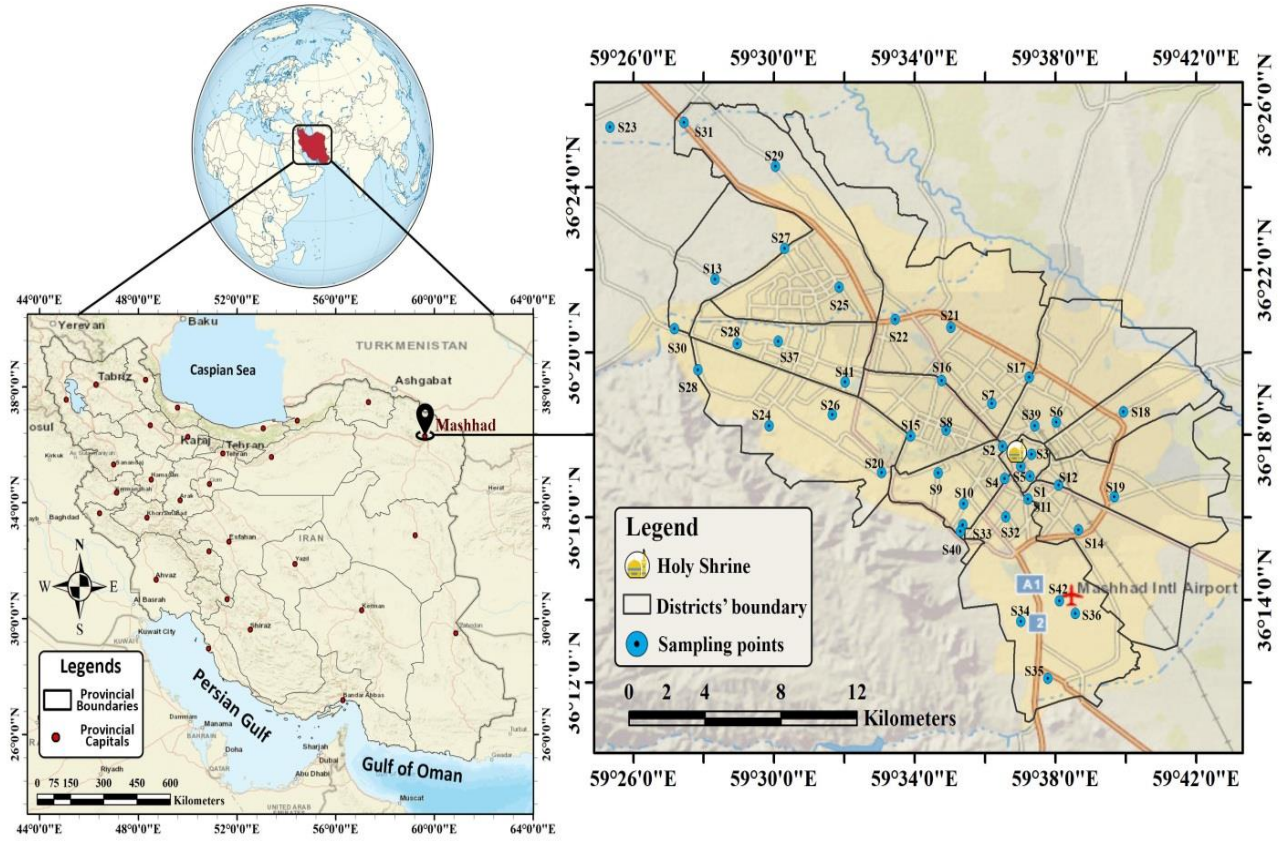

Fig. 1. Study area and sampling site locations in the city of Mashhad, Northeastern Iran.

2.2. Material and chemicals

To measure PAHs concentrations, a mixture of the following 16 USEPA priority PAHs was used: Naphthalene (Nap), Acenaphthylene (Acy), Acenaphthene (Ace), Fluorene (Flo), Phenanthrene (Phe), Anthracene (Ant), Fluoranthene (Flt), Pyrene (Pyr), Benzo(a)anthracene (BaA), Chrysene (Chr), Benzo(b)fluoranthene (BbF), Benzo(k)fluoranthene (BkF), Benzo (a) pyrene (BaP), Indeno (1,2,3,cd), pyrene (InP), Dibenzo(a,h)anthracene (DahA), Benzo(ghi)perylene (BghiP). For quality control of the protocol, a mixture of recovery surrogates containing 200 μg kg^{-1} of naphthalene-d_8, phenanthrene-d_{10}, chrysene-d_{12}, and perylene-d_{12} was used as the internal standard. The standard solutions were obtained from Sigma-Aldrich, and the organic reagents including acetone, methanol, dichloromethane, and n-hexane used during the analysis were HPLC-grade and purchased from Merck (Darmstadt, Germany).

2. 3. PAH extraction and analysis

The PAHs were extracted and measured based on the method described by Zakariaa et al (2000), with some modifications. The dust samples were Soxhlet extracted using 100 ml of dichloromethane for 12 h (Zakaria et al., 2000). About 5 g dust collected at each station was freeze dried for 72 h and then 100 µL of the surrogate internal standard mixture (i.e., naphthalene-d_8, phenanthrene-d_{10}, chrysene-d_{12}, and perylene-d_{12}) was added to the samples. The dust samples were Soxhlet with 100 mL dichloromethane for 12 hours. The obtained supernatant was evaporated using a rotary. The concentrated extract was further evaporated to 0.1 ml using a nitrogen blowing instrument and then kept in a refrigerator at 4 °C. To remove any organic contaminant, the glassware were rinsed with methanol, acetone, and hexane and then kept in an oven at 60 °C for 2 h.

The concentrations of PAHs were determined using an Agilent gas chromatography (Model 7890A) coupled to a quadrupole mass spectrometer (GC–MS; Model 5975C MSD). The GC-MS instrument was equipped with a fused silica capillary column covered with 5% phenylmethyl siloxane (Agilent DB-5MS). The target PAHs were detected according to their m/z and retention times in the selected ion monitoring (SIM) mode (Aceves and Grimalt, 1993; Azimi et al., 2018). The GC-MS condition was optimized at 70eV ionization potential with the source at 200 °C and electron multiplier voltage at ~ 2000 eV. The injection port was maintained at 310 °C and operated in split-less mode (splitter valve off by 1 min). The column temperature was adjusted at 70 °C for 2 min, increased to 150 °C (30 °C min^{-1}) and then to 310 °C (4 °C min^{-1}), maintaining the isothermal conditions for 10 min. Helium was used as the carrier gas at a constant pressure of 15 psi.

2.3. Method validation

The quality assurance and quality control of the method used for measuring the PAHs levels were determined using the laboratory blanks and spiked recoveries during the sample

collection, preservation, and analysis (Bakhtiari et al., 2009; Zakaria et al., 2000). About 200 µl of the above-mentioned surrogate internal standard, containing 5 ppm of a mixture of naphthalene-d_8, acenaphthene-$d1_0$, phenanthrene-d_{10}, chrysene-d_{12}, and perylene-d4, was spiked to determine the recovery of the target PAHs. Constituents of the spiked surrogate internal standard demonstrated a recovery between 87% and 104%. PAHs showed a recovery between 87% and 104% in summer and 84% and 107% in winter. The protocol performance was assessed using relative standard deviation (RSD); the RSD was measured through analyzing five replicates of the same sample and showed a value of <9% for all of the PAHs.

2. 4. Source apportionment techniques

2. 4.1. Diagnostic ratios and Principal component analysis (PCA)

Diagnostic ratios of PAHs including Phe/Ant, BbF/BkF, BaP/BghiP, InP/BghiP, Pyr/BaP, BaA/(BaA+Chr), Flt/(Flt+Pyr) and InP/(InP+BghiP) were used to identify the pyrogenic and anthropogenic possible sources of PAHs in the street dust samples (Moeinaddini et al., 2014b; Mon et al., 2020; Ravindra et al., 2008). Principal component analysis (PCA) was applied to identify patterns and associations of individual PAHs. Kaiser-Meyer-Olkin (KMO) test and Bartlett test were used to determine the adequacy of data for Factor Analysis (FA); KMO value of >0.6 was considered suitable for FA of the PAHs in summer and winter (Moeinaddini et al., 2014b). Moreover, Varimax rotation besides PCA (eigenvalues >1) was used for source grouping, and PAHs with a factor loading of >0.5 were selected as the representative species of the factor (Ravindra et al., 2008; Wang et al., 2011a).

2. 4.2. Positive matrix factorization (PMF)

The US EPA's PMF model software (version 5.0: https:// www.epa.gov / sites / production / files / 2015 - 02 / documents / pmf_5.0_user_guide.pdf) was also used to identify the source apportionment and to quantify the major dust sources in the study area (USEPA, 2014). Total concentrations of PAHs were used as input data. The uncertainties of the target PAHs were

calculated according to the values of method detection limits (MDL) (2014), see more details in the supplementary file (section A1). The model was bootstrapped by 100 runs with a minimum correlation of 0.7, and random seed. Three to seven factors were assessed and the optimal factor was selected based on the Q value slope versus the factors' numbers (Javed et al., 2019; Lang et al., 2015; Teixeira et al., 2015).

2. 5. Human health and cancer risk assessment

The toxic equivalency factor (TEF) was used to estimate the potential carcinogenic risk of the target PAHs in the dust samples. To this end, Benzo[a]pyrene (BaP) was applied as the reference molecule with a TEF value of 1, and this index was determined for other PAHs (Nisbet and Lagoy, 1992). The toxic equivalent quantities (TEQs) for the street dust was calculated as follows:

$$\text{TEQs} = \sum C_i \times TEF_i \quad (1)$$

Where Ci is the concentration of PAHi and TEFi is the corresponding toxic equivalency factor value. TEF values of the measured PAHs were adopted from two previously published reports, see Table 1 (Malcolm and Dobson, 1994; Nisbet and Lagoy, 1992).

The potential cancer risk of the measured PAHs was determined using the incremental lifetime cancer risks from the main exposure routes including ingestion, inhalation, and dermal contact (ILCRs; equations 2–5) (EPA, 1991). The ILCRs of ingestion, dermal contact, and inhalation were calculated using the following equations (Ma et al., 2017; Martuzevicius et al., 2011):

$$\text{ILCRs}_{\text{Ingestion}} = \frac{\text{CS} \times \left(\text{CSF}_{\text{ingestion}} \times \sqrt[3]{\frac{\text{BW}}{70}}\right) \times \text{IR}_{\text{ingestion}} \times \text{EF} \times \text{ED}}{\text{BW} \times \text{AT} \times 10^6} \quad (2)$$

$$ILCRs_{Dermal} = \frac{CS \times \left(CSF_{Dermal} \times \sqrt[3]{\frac{BW}{70}}\right) \times SA \times AF \times ABS \times EF \times ED}{BW \times AT \times 10^{6}} \quad (3)$$

$$ILCRs_{Inhalation} = \frac{CS \times \left(CSF_{inhalation} \times \sqrt[3]{\frac{BW}{70}}\right) \times IR_{inhalation} \times EF \times ED}{BW \times AT \times PEF} \quad (4)$$

$$\text{Carcinogenic Risk} = ILCR_{Ingestion} + ILCR_{Dermal} + ILCR_{Inhalation} \quad (5)$$

Where CS is the sum of converted PAH concentrations based on toxic equivalents of BaP using the TEFs; CSF, cancer slope factor (mg kg^{-1} day^{-1}); BW, body weight (kg); AT, average life span (day); EF, exposure frequency (day $year^{-1}$); ED, exposure duration (year); $IR_{Inhalation}$, inhalation rate (m^3 day^{-1}); $IR_{Ingestion}$, dust intake rate (mg day^{-1}); SA, dermal surface exposure (cm^2); AF, dermal adherence factor (mg cm^{-2}); ABS, dermal adsorption fraction; and PEF, particle emission factor (m^3 kg^{-1}). Table S1 shows the other parameters (supplementary section).

3. Results and discussion

3.1. PAH concentrations and spatial distribution

Total concentration of the 16 PAHs (ΣPAH) demonstrated a range between 1,206.21-9,138.96 µg kg^{-1} dw (Avg. 2771.19 µg kg^{-1} dw) and between 1,005-7864.77 µg kg^{-1} dw (Avg. 2369.89 µg kg^{-1} dw) in the dust samples collected in summer and winter, respectively (Table 1 and Fig. 2). Irrespective of this seasonal difference, the target PAHs exhibited a similar proportion among all of the locations (Fig. 2). Six locations (S5, S36, S42, S39, and S40) of the study area exhibited higher ΣPAH levels in summer. These locations are the nearby regions with high traffic density and air pollution, including underpass of the holy shrine (Imam Reza), airport, railway station, and bus terminal. The higher levels of PAHs at these locations could be ascribed to the public transport systems and passenger vehicles of the pilgrims and tourists (over 20 million) being annually attracted to Mashhad city in summer. According to the

transportation statistics annual report of Mashhad, fuel consumption (gasoline and diesel) is significantly increased during summer, due to the influx of summer tourists and pilgrims (Talebian and Riza, 2020). However, the lowest levels of ΣPAHs were measured in the residential locations and this could stem from the combustion of natural gas that produces lower PAHs in comparison to solid and liquid fuels. The levels of dust-bound ∑PAHs were higher than those reported previously for some urban areas of Iranian cities such as Bushehr (1,116.2 µg kg^{-1} dw, (Keshavarzi et al., 2020)), Isfahan (1,074.6 µg kg^{-1} dw, (Soltani et al., 2015)) and Ahvaz (1,031.5 µg kg^{-1} dw, (Najmeddin and Keshavarzi, 2019)) but lower than those measured in Lanzhou, China (Jiang et al., 2014), Tokyo, Japan (Takada et al., 1991), Newcastle, UK (Lorenzi et al., 2011), Cairo, Egypt (Hassanien and Abdel-Latif, 2008) and Ulsan, Korea (Dong and Lee, 2009) (See Table S2; supplementary data).

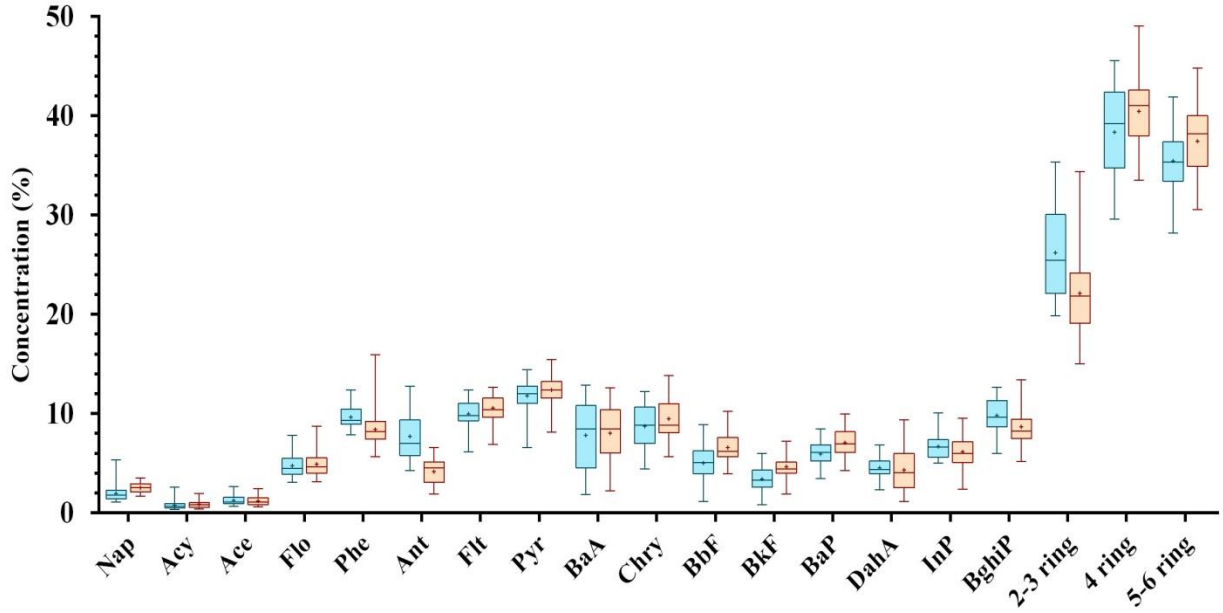

Fig. 2. Box-plot of percentage concentration for the PAHs in Mashhad street dust samples in summer (blue) and winter (red).

The ∑PAHs in dust samples exhibited higher levels when compare to those of previous reported for some urban areas of Egypt, 27-379 µg kg^{-1} (Mostafa et al., 2009); Kuala Lumpur, 116-332 µg kg^{-1} (Omar et al., 2002); and Jalalabad, 288 µg kg^{-1} (Khpalwak et al., 2019) and

forest areas of the Alps (77-501 µg kg^{-1} , 185 µg kg^{-1}) (Belis et al., 2009) but showed lower concentrations than those measured in Guangzhou, 840-12400 µg kg^{-1}(Wang et al., 2011b); Xian, 500-48000 µg kg^{-1} (Wang et al., 2016); and Nepal, 747-4910 µg kg-(Yadav et al., 2018).

Table 1. Concentration, statistical parameters, and toxicity aspects of PAHs in the street dust of Mashhad in summer and winter.

		Summer					Winter		
Compound	TEF	Min	Max	Mean	Median	SD	Min	Max	Mean
Nap	0.001	28.49	271.73	53.45	40.97	39.06	33.45	214.74	57.65
Acy	0.001	11.47	237.24	23.59	15.71	34.62	11.04	156.04	21.36
Ace	0.001	22.14	215.56	35.01	27.06	29.68	17.07	194.41	29.05
Flo	0.001	77.95	713.56	130.20	116.68	94.83	72.09	588.20	113.79
Phe	0.001	126.64	995.51	268.85	261.77	138.03	90.79	1254.83	207.01
Ant	0.01	129.43	797.05	199.83	181.67	99.13	41.18	297.51	95.59
Flt	0.001	132.58	563.98	266.28	253.28	88.00	123.82	545.07	241.53
Pyr	0.001	135.99	985.05	327.02	299.15	152.91	128.84	793.45	289.84
BaA	0.1	25.24	859.03	242.54	212.99	176.26	32.29	706.06	201.98
Chry	0.01	100.05	611.13	239.86	214.68	109.55	108.80	644.63	222.67
BbF	0.1	13.71	502.25	146.24	134.32	88.98	54.73	358.18	150.86
BkF	0.1	11.25	473.70	99.39	93.05	73.89	42.22	329.38	107.98
BaP	1	51.32	641.24	168.96	166.49	95.97	52.93	517.05	169.15
DahA	1	69.11	223.39	118.86	115.57	38.19	22.87	360.54	108.66
InP	0.1	63.42	479.63	182.81	175.88	75.02	54.70	272.52	139.45
BghiP	0.01	107.28	568.89	268.35	244.98	111.27	74.92	715.52	212.36
∑PAHs		1206.21	9138.96	2771.19	2571.50	1294.89	1005.00	7864.77	2369.86
2–3 rings		19.87	35.35	26.19	25.44	4.47	15.01	34.40	22.09
4 rings		29.60	45.56	38.35	39.26	4.33	33.54	49.04	40.42
5-6 rings		28.21	41.90	35.46	35.33	3.27	30.58	44.81	37.45
TEQ		150.32	1350.46	420.66	409.07	198.36	127.07	901.96	371.81

The observed differences in the dust–bounded PAHs concentrations among these areas could be associated with the economical level, industrial structure, traffic density, population, precipitation, meteorological condition, and the particle size of street dust (Hussain et al., 2015) (See Table S2; supplementary data).

Higher levels of PAHs were detected in summer than that of in winter, and this finding could be linked to the heavy washout in winter, thereby eliminating the adsorbed PAHs from street surface (Gope et al. 2018). According to ∑PAHs concentrations, soil is categorized into four classes as follows: uncontaminated, ∑PAHs < 200 ng g^{-1}; weakly contaminated, ∑PAHs = 200–600 ng g^{-1}; contaminated, ∑PAHs = 600–1000 ng g^{-1}; and heavily contaminated, ∑PAHs

241 > 1000 ng g^{-1} (Maliszewska-Kordybach, 1996). Accordingly, the street dust in the studied area
242 of Mashhad could be classified as heavily PAHs contaminated dust.

243 **3.2. Composition of dust PAHs**

244 PAHs composition of street dust in urban environments could reveal the sources and potential
245 risk to human health. According to their molecular structure, the measured PAHs were
246 categorized into three groups and exhibited the seasonal percentages in the order of 4 rings
247 (summer, 38.35%; winter, 40.42%)> 5–6 rings (summer, 35.46 %; winter, 37.45%)> and 2–3
248 rings (summer, 26.19%; winter, 22.09%) (Table 1 and Fig. 2.). Possible explanations for this
249 might be ascribed to higher volatility of the 2-3 ring molecules than high molecular weight
250 (HMW) PAHs as well as higher tendency of HMW-PAHs to adhere to street dust (Chung et
251 al., 2007; Keshavarzi et al., 2020; Wang et al., 2011a). Moreover, the observed higher levels
252 of HMW-PAHs could reveal their sources from petroleum fuel combustion (Liu et al., 2007;
253 Najmeddin et al., 2018; Wang et al., 2017). In accordance with the present results, previous
254 studies have detected higher concentrations of HMW-PAHs in street dust from various urban
255 areas. The findings were largely attributed to pyrogenic sources (especially vehicle exhaust
256 emissions) (Bandowe and Nkansah, 2016), non-exhaust sources (e.g., brake wear, asphalt,
257 petroleum, and oil emissions from automobiles and motorbikes) (Majumdar et al., 2012), and
258 biomass burning (Tobiszewski and Namieśnik, 2012).

259 Among the sampling locations, the street dust collected at S5 displayed different PAHs
260 composition (about 68%; 2-3 rings and 4 rings). The 2–3 ring molecules demonstrated the
261 highest percentage (35.35% in summer and 34.40% in winter), followed by 4 rings (33.04% in
262 summer and 34.19% in winter), and 5–6 rings (31.61% in summer and 31.40% in winter). This
263 result may be explained by the fact that this station (the holy shrine underpass) always undergo
264 heavy automobile traffic where vehicles slow down or stop whereupon their engines run at

lower temperatures (Song et al., 2005). The holy shrine underpass receives no sun radiation, especially UV radiation and have lower temperature in comparison with the surrounded streets. Accordingly, the dust-bounded PAHs in the underpass are subjected to lower photo-degradation during both summer and winter (Škrbić et al., 2019).

3.4. PAHs sources

The characteristic ratios of Flt/Flt+Pyr, Ant/Ant+Phe, InP/InP+Bghi, BaA/BaA+Chr, BbF/BkF, BaP/BghiP, InP/BghiP, and Pyr/BaP are presented in Table S3 and Fig. 3. The values of <0.4, 0.4–0.5, and >0.5 for Flt/Flt+Pyr indicate the presence of petroleum, liquid fossil fuel combustion, and biomass and coal combustion sources, respectively, (Jiang et al., 2014; Tobiszewski and Namieśnik, 2012).

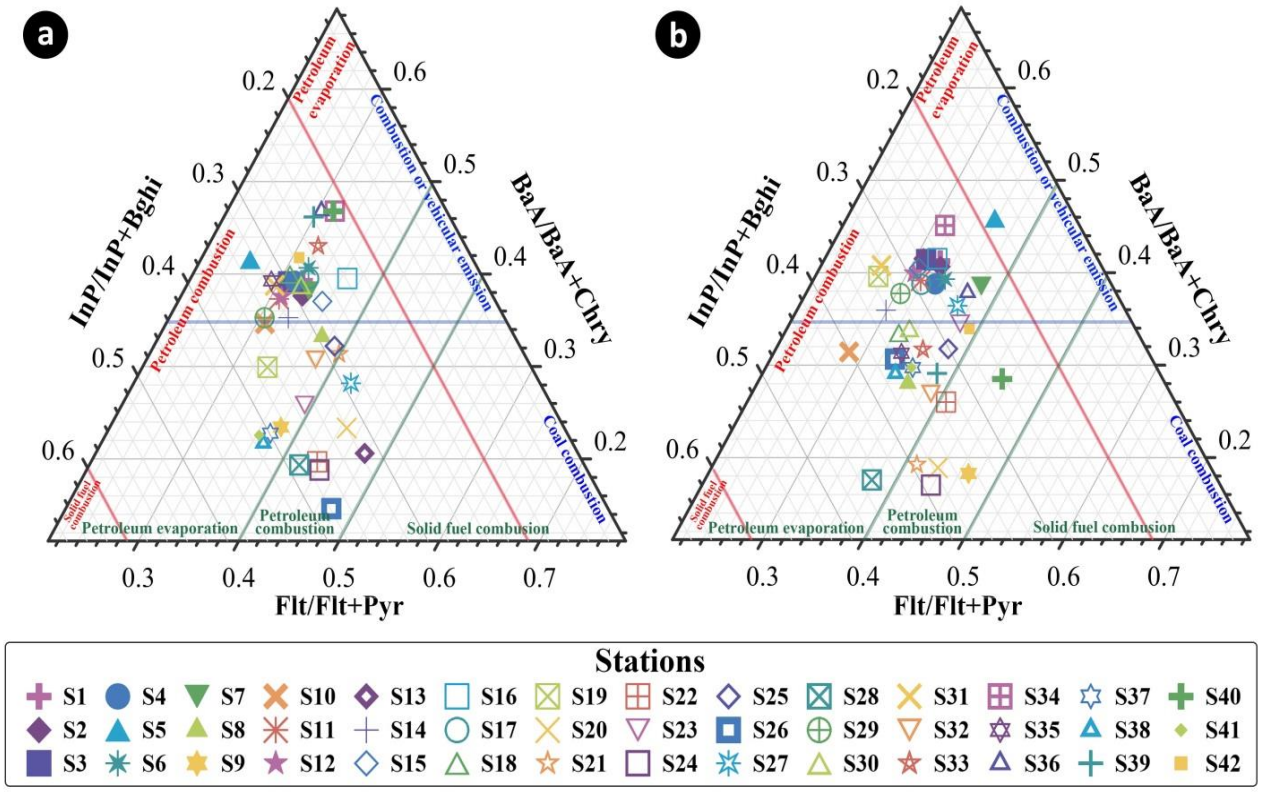

Fig. 3. Triangular diagram of diagnostic ratios based on PAH parents and isomers for source identification in Mashhad street dust samples **(a)** in summer and **(b)** winter

BaA/(BaA+Chr) ratios of <0.2, 0.2-0.35, and >0.35, respectively, reflect the origin of PAHs from petrogenic material, coal combustion, and vehicular emission. In the present study, Flt/Flt+Pyr showed a value of 0.46 for the collected dust samples in both summer and winter and suggested that liquid fossil fuel combustion was the major pyrogenic source of the PAHs. The BaA/(BaA+Chr) ratio of 0.46 in summer and 0.45 in winter revealed the strong contribution of vehicles to PAHs emission in the study area. InP/(InP+BghiP) ratio in both seasons showed a value of 0.41, suggesting the meaningful contribution of vehicles as well as diesel and petroleum combustions as the emission sources in the area (Jafarabadi et al., 2017; Jiang et al., 2014; Yunker et al., 2002). Further three indices (BbF/BkF ratio of >0.5; BaP/BghiP ratio of >0.5; and Pyr/BaP ratio of >1) also confirmed the association between diesel/gasoline combustion and the street dust PAHs (Table S3) (Caricchia et al., 1999), and all of the ratios highlighted pyrogenic materials, especially liquid fossil fuel combustion, as the major sources of the target PAHs in Mashhad city. Cluster analysis was performed to identify the temporal correlation among the PAHs and/or sampling stations (Fig. 4). Due to their different scales, the variables (i.e., PAHs and stations) were standardized and illustrated by a dual dendrogram. The horizontal and vertical axes, respectively, illustrate the clustering of sampling sites according to PAHs and the similarities among the stations. The detected PAHs showed a fairly similar distribution across the area in both summer and winter. Cluster analysis distinguished two major groups of detected PAHs in both seasons. The low molecular weight PAHs with 2–3 rings (Acy, Ace, Flo, Phe, Nap, and Ant) that are abundant in petrogenic sources and mainly produced by petroleum sources were clustered into a separate group. However, the molecules with 4 rings (BaA, Flt, Chry, and Pyr) and 5-6 (BbF, BkF, Bap, DahA, InP, and BghiP) rings were categorized in another group and these PAHs are usually detected in pyrogenic source, e.g., combustion of coal, wood, vehicle fuel and waste tire (Liu et al., 2009). As to sampling site clustering, two main groups were observed; location S5 (group 1)

was related to the dust samples collected from the underpass of the holy shrine and showed a great distance from the other groups or subgroups. Subgroup 2 demonstrated the sites around the city across which diesel-powered trucks and gasoline-powered private cars pass all day and all night. Subgroup 3 showed higher PAHs concentrations than subgroups 1 and 2 and was related to the city center with dense traffic by gasoline-fuelled cars as well as the airport, bus terminal, and railway station. Subgroup 4 covers the areas with medium and low traffic densities, especially residential buildings. The cluster analysis revealed a close correlation between the PAHs distribution pattern in the street dust and regional traffic status.

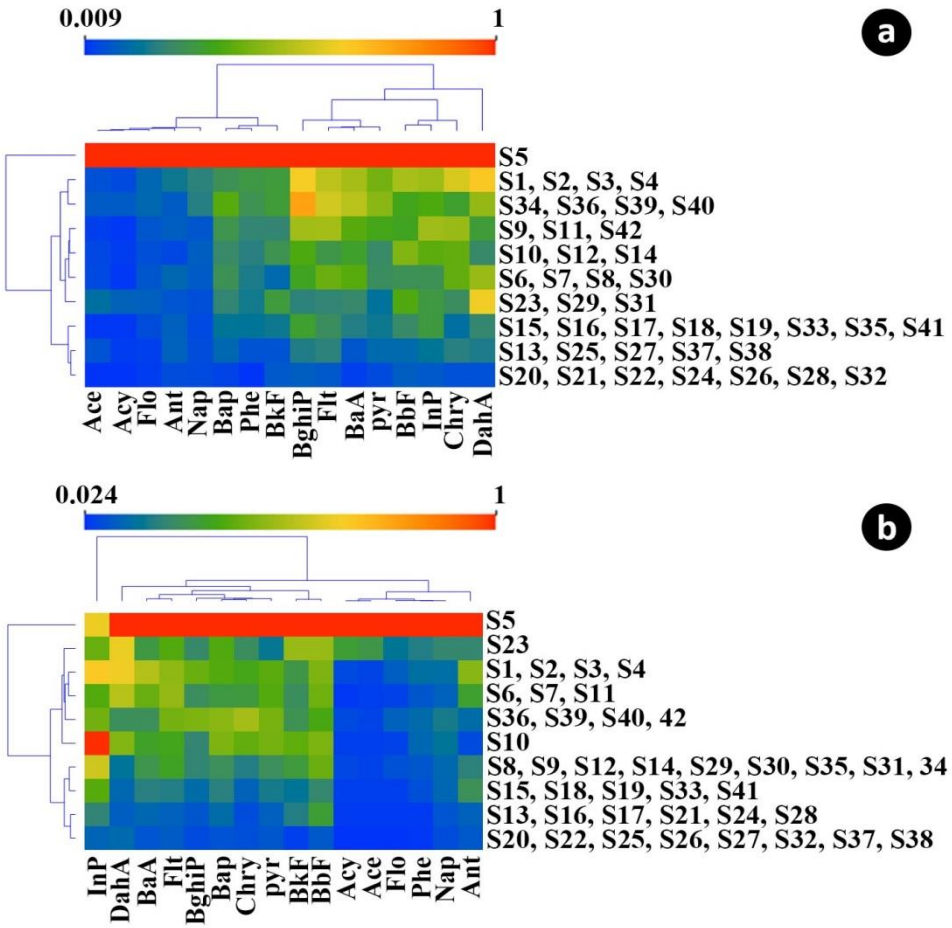

Fig. 4. Heat-map (DHCA) showing correlations between PAHs and street dust samples **(a)** in summer and **(b)** winter, from Mashhad, Northeast Iran. Note: Samples are labelled and clustered at columns and rows as highest value (light to dark red), moderate value (light to dark green and yellow) and lowest value (light to dark blue).

3.3. Source apportionment using PCA and PMF

PCA has been used to locate the major sources of air pollutants. In this research, PCA with the varimax rotation classified the 16 PAH congeners into three factors that accounted for 91% and 89% of the total data variance in summer and winter, respectively (Table 2 and Fig. 5). Factor 1 contributes 40% in summer and 39.01% in winter of the total variance and shows a strong association between Nap, Acy, Ace, Flo, Phe, Ant, BkF, and Bap, indicating the presence of fossil fuel, biomass and oil combustion sources (Khalili et al., 1995; Larsen and Baker, 2003; Zhang et al., 2017) and Flo, Phe and Ant as markers of oil combustion (Caricchia et al., 1999; Dong and Lee, 2009; Harrison et al., 1996). In accordance with the present results, previous studies have demonstrated relatively high factor loadings for Ace, Acy, and Phe from wood and fossil fuels such as liquefied petroleum gas and coal combustion (Ghanavati et al., 2019; Guo et al., 2003; Škrbić et al., 2019; Soltani et al., 2015) and identified BkF and BbF as markers of fossil fuel combustion (Park et al., 2002; Sulong et al., 2019; Tobiszewski and Namieśnik, 2012). Factor 2 accounts for 34.33% of the total variance in summer and 34.27% in winter and is characterized by high loadings of HMW-PAHs (Chr, BaA, Flt, Pyr, BaP, InP, and BghiP), suggesting vehicle-related sources such as diesel and gasoline [33, 67, 74, 75, 76, 77]. Factor 3 accounts for 16.76% of total variance in summer and 15.67% in winter and was correlated with HMW-PAHs (BaA, Chr, BbF, DahA, and InP). The third factor recognized the proportion of natural gas combustion and steel and power plants (Moeinaddini et al., 2014a; Ravindra et al., 2008; Yang et al., 1998). Due to lower pressure of natural gas in cold seasons, industrial plants (station 23) in Mashhad mainly utilize gasoline instead of natural gas, thereby emitting higher levels of PHAs during winter.

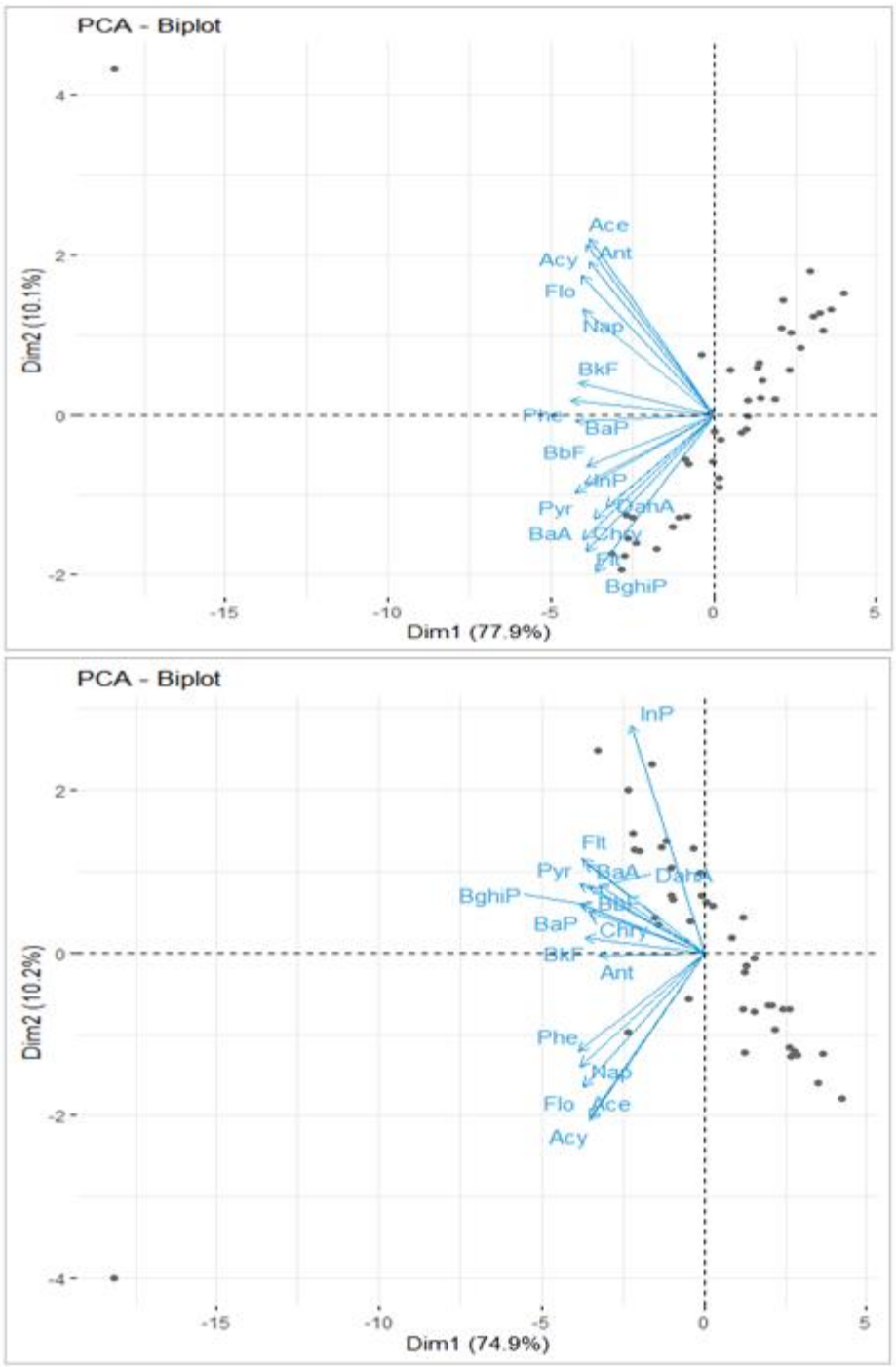

Fig. 5. Biplot illustrating PCA for PAHs in street dust samples **(a)** in summer and **(b)** winter, from Mashhad, Northeast Iran.

Moreover, the residents mainly use natural gas to heat houses and offices in winter. These results seem to be consistent with other research which attributed high concentration of BbF to heavy oil combustion and DahA to power plants as well as BaP, BaA, BeP to steel industry (Wang et al., 2011a). The PCA analysis ranked liquid fossil fuel combustion and vehicular

emission as the first sources of the PAHs in the study area and identified similar pattern for their concentrations in summer and winter.

Table 2. The results of principal component analysis (PCA) for PAHs in summer and winter.

	PAH factor					
	Summer			Winter		
	1	2	3	1	2	3
Nap	***0.82***	0.42	0.22	***0.87***	0.37	0.26
Acy	***0.93***	0.25	0.23	***0.93***	0.19	0.28
Ace	***0.93***	0.22	0.23	***0.92***	0.20	0.28
Flo	***0.90***	0.34	0.24	***0.90***	0.31	0.26
Phe	***0.68***	***0.59***	0.37	***0.84***	0.39	0.32
Ant	***0.79***	0.28	***0.52***	0.45	0.30	***0.75***
Flt	0.30	***0.84***	0.36	0.40	***0.74***	0.45
Pyr	0.48	***0.79***	0.33	0.49	***0.75***	0.33
BaA	0.35	***0.73***	***0.52***	0.37	***0.66***	***0.56***
Chr	0.32	***0.59***	***0.58***	0.42	***0.67***	***0.51***
BbF	0.46	0.49	***0.63***	0.47	***0.74***	0.22
BkF	***0.68***	0.48	0.42	***0.61***	***0.68***	0.15
BaP	***0.63***	***0.65***	0.32	***0.55***	***0.74***	0.25
DahA	0.26	0.37	***0.80***	0.30	0.45	***0.75***
InP	0.43	***0.60***	***0.53***	-0.10	***0.84***	0.22
BghiP	0.23	***0.92***	0.21	0.50	***0.69***	0.35

[a] Values in bold/italics are for factor loading values >0.5 and indicate important factors for each component

As a receptor-based model, PMF has been widely used for source apportionment of various environmental pollutants (Gope et al., 2020; Teixeira et al., 2013; Xia et al., 2020). The optimal number of factors for PMF analysis was determined by resetting the number of sources (from 3 to 7) and produced a Q value close to the number of freedom degrees, indicating an appropriate uncertainty in the modeling input. The factors provided the minimum Q (Robust)/ Qexp value were considered as the optimum ones. Four appropriate factors were identified by the PMF model. The PMF model demonstrated different results from those observed by PCA. Regardless of season, PMF model displayed four major emission factors for the target PAHs: 1) gasoline combustion, 2) petrogenic source, 3) diesel combustion, and 4) natural gas, fossil fuel, and biomass combustion (Fig. 6a).

In summer, Factor 1 displayed high loads of Flt, Pyr, BaA, Chr, BaP, BbF, InP, and BghiP (about 34% of the total PAHs) (Fang et al., 2004; Khalili et al., 1995; Zhen et al., 2020). Petrogenic source (Factor 2) emitted 7.5% of the total d PAHs, characterized by high Nap, Acy,

Ace, and Flo (2-3 ring) [29]. The third factor was predominately composed of Nap, Acy, Ace, Flo, Ant, Flt, Chr, DahA, and BghiP (about 30.2% of the total PAHs) in summer, suggesting diesel combustion as the third source (Hassanien and Abdel-Latif, 2008; Keshavarzi et al., 2020; Moeinaddini et al., 2014b; Ravindra et al., 2006). Factor 4 was predominately weighted in Nap, Acy, Ace, Flo, BbF, and BkF (about 28.3% of the total PAHs), indicating natural gas, fossil fuel, and biomass combustion as the main sources (Harrison et al., 1996; Park et al., 2002; Škrbić et al., 2019; Wang et al., 2011a). Ant is the typical marker for natural gas combustion (Harrison et al., 1996) whereas Acy, Ace, and Flo are often emitted from diffuse point sources (Ghanavati et al., 2019; Moeinaddini et al., 2014a). For winter, fairly similar emission sources of the PAHs (fossil fuel and biomass combustion, diesel combustion source, natural gas combustion and stationary sources, gasoline combustion source) were recognized by the model (Fig. 6b). Factor 1 was characterized by high loadings of Ant, Phe, BaA, Chr, BaP, BbF, BkF, and DahA (21.2% of the ∑PAHs), which are considered as good markers of natural gas, fossil fuel and biomass combustion (Harrison et al., 1996; Park et al., 2002; Škrbić et al., 2019; Tobiszewski and Namieśnik, 2012). Factor 2 was predominately loaded on Nap, Acy, Ace, Flt, Pyr, Chr, BaP, DahA, and BghiP (about 37.7% of the ∑PAHs) which were identified as typical products of diesel combustion (Fang et al., 2004; Khalili et al., 1995; Simoneit, 1984; Zhen et al., 2020). The third source was mostly associated with Nap, Acy, Ace, Flo, and Phe (about 11.9% of the ∑PAHs), suggesting that source 3 might represent the petrogenic source. Source 4 had significant loadings on Ant, Flt, Pyr, BaA, BbF, BkF, InP, and BghiP (about 29.1% of the ∑PAHs) which are usually associated with gasoline combustion (Fang et al., 2004; Khalili et al., 1995; Ravindra et al., 2008). Although the source apportionment technique showed extremely similar potential sources PAHs in summer and winter, the contribution of some sources was different between the two seasons. Gasoline combustion displayed a greater contribution in summer than that of in winter, and this could

396 stem from the significant presence of tourist's car in summer. However, diesel combustion
397 showed a larger proportion in PAHs emission in winter because the combined cycle power
398 plants use both natural gas and gasoline to produce electricity when the pressure of natural gas
399 in supplying pipelines is low.

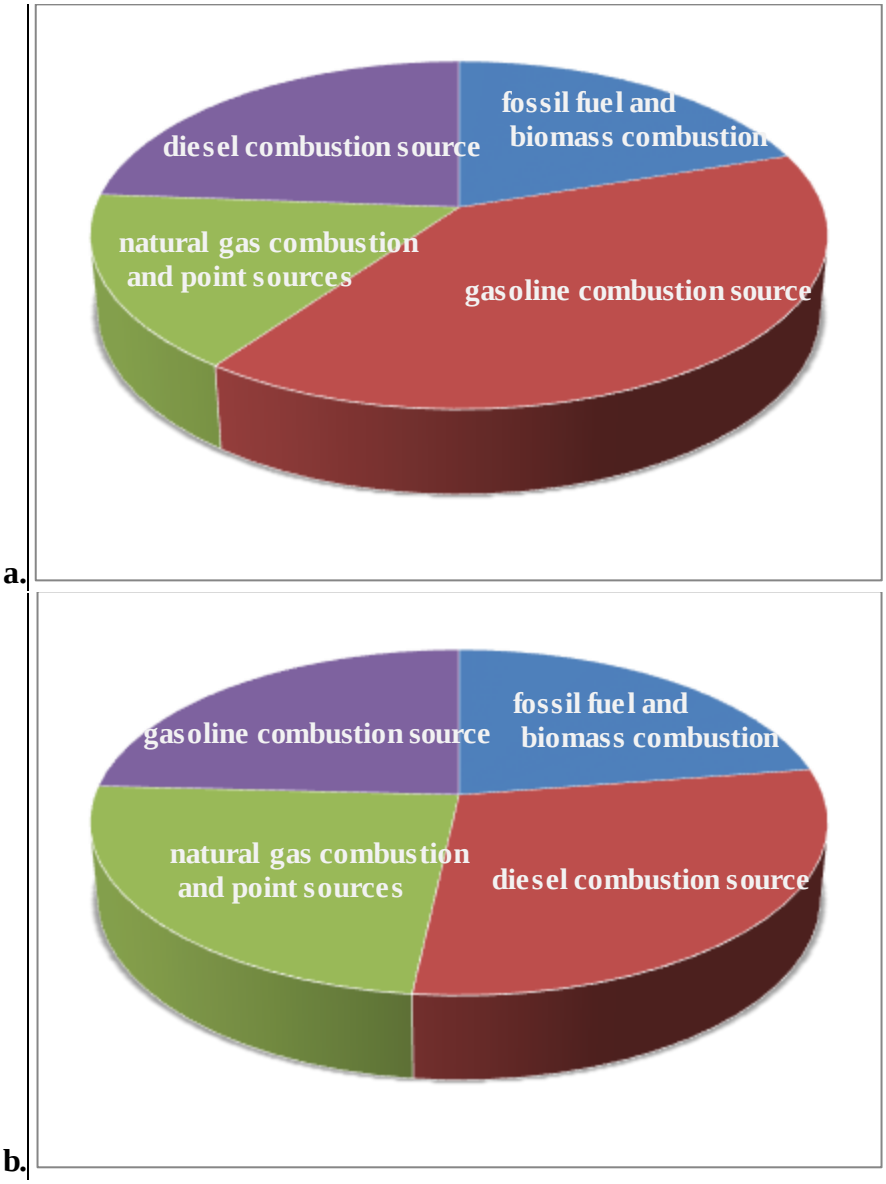

400

401 **Fig. 6.** contribution (%) of each factor to total PAH burden in street dust and Fingerprinting of
402 each PAHs in street dust of Mashhad, Iran in summer **(a)** and winter **(b)**.

403 **3.4. Health risk assessment of street dust PAH contamination**

404 Due to the high toxicity of PAHs to human health, the ever-increasing concentration of these
405 molecules has raised concerns worldwide. Exposure to dust-bounded PAHs through different

406 pathways including ingestion, dermal contact, and inhalation is inevitable in urban
407 environments [29]. The present study assessed the potential toxicity of 16 priority PAHs in the
408 street dust of Mashhad city. TEQ of the dust samples was determined according to TEF [47].
409 To manage the risk of dust-bounded PAHs in urban areas, it is recommended to reduce the
410 accumulation of HMW PAHs, especially DahA and BaP, on street surface (Ma et al., 2017).
411 ILCR index was applied to estimate the potential cancer risk via simultaneous
412 inhalation/dermal/oral exposure to the street dust PAHs in Mashhad. ILCR values of $\leq 10^{-6}$ and
413 $>10^{-4}$, respectively, indicate negligible and high potential cancer risk (Liao and Chiang, 2006).
414 According to the daily exposure levels in both summer and winter, the ingestion, dermal, and
415 inhalation ILCRs for adults and children were estimated, respectively, about 10^{-7}, 10^{-7}, and 10^{-11},
416 suggesting lower carcinogenic risk of the PAHs through inhalation (Table 3). The ILCR
417 ingestion showed higher value for children as compared to the other routes, and it has been
418 speculated that hand-to-mouth activity of children makes them the most sensitive
419 subpopulation to PAHs (Jiang et al., 2014; Xu et al., 2016). Moreover, the street dust PHAs
420 showed higher potential to cause cancer through dermal exposure, whereas the potential risk
421 via inhalation was almost negligible. Overall, these findings highlight the carcinogenic risk of
422 the PAHs (with ILCR of 10^{-6}) for the permanent residents and tourists of Mashhad, and the
423 value was higher than the baseline of acceptable risk. The children and adults suffer long-term
424 dermal and ingestion exposure to fairly high potential carcinogenic levels of street dust PAHs,
425 especially in summer. Similar findings were previously reported about the relative significance
426 of human exposure pathways to street dust PAHs (Gope et al., 2018; Jiang et al., 2014; Soltani
427 et al., 2015). Seasonal variation in the concentration of street dust PAHs should be presumed
428 to prove accurate risk characterization. Higher levels of PAHs were measured in summer than
429 that of in winter, and this finding may be explained by the heavy washout and runoff in winter
430 and thus removing the street particulates and the adsorbed PAHs.

Table 3. The incremental lifetime cancer risk (ILCR) for children and adults in street dust of Mashhad in summer and winter.

	Exposure pathways	Children				Adul		
		$ILCR_{ingestion}$	$ILCR_{inhalation}$	$ILCR_{Dermal}$	Cancer risk	$ILCR_{ingestion}$	$ILCR_{inhalation}$	
Summer	Min	3.70E-07	7.18E-12	4.61E-07	8.31E-07	2.89E-07	2.24E-11	5
	Max	3.32E-06	6.45E-11	4.14E-06	7.47E-06	2.60E-06	2.01E-10	4
	Mean	1.08E-06	2.09E-11	1.34E-06	2.42E-06	8.41E-07	6.52E-11	1
Winter	Min	3.13E-07	6.06E-12	3.90E-07	7.03E-07	2.44E-07	1.89E-11	4
	Max	2.22E-06	4.31E-11	2.77E-06	4.99E-06	1.73E-06	1.34E-10	3
	Mean	9.15E-07	1.77E-11	1.14E-06	2.06E-06	7.15E-07	5.54E-11	1
Both season	Min	3.13E-07	6.07E-12	3.90E-07	7.03E-07	2.44E-07	1.89E-11	4
	Max	3.32E-06	6.45E-11	4.14E-06	7.47E-06	2.60E-06	2.01E-10	4
	Mean	9.96E-07	1.93E-11	1.24E-06	2.24E-06	7.78E-07	6.03E-11	1

4. Conclusion

This research investigated the occurrence and distribution of USEPA regulated 16 PAHs in street dust of Mashhad city, assessed their concentrations and health risk to human health, as well as identified the contamination sources. Higher levels of ∑PAHs were measured in the street dust samples collected in summer, which could stem from massive summer tourist and pilgrim flows and, in turn, heavy traffic and high levels of the PAHs (especially 4-ring ones) in the area around the holy shrine. The diagnostic ratios analysis, PMF model, and PCA suggested that PAHs in the surface street dust samples were originated from diesel and gasoline combustion, petrogenic sources, and fossil fuel and natural gas combustion. The ILCR values indicated high potential risk of the PAHs for the citizens and tourists, mainly via dermal exposure. Taken together, these results suggest that diesel- and gasoline-powered vehicles are the predominant emitting sources of the PAHs in Mashhad, and this research has shed a contemporary light on the contentious issue of persistent organic pollutants caused by diesel- and gasoline-powered vehicles as well as diesel and petroleum combustions. Technical improvement in the performance of diesel and gasoline vehicles could reduce the pollution, and the findings might be useful to manage the environmental air quality in similar urban areas across the world, especially World Heritage Sites, or those with high tourist attraction. The

observed high concentrations of ∑PAHs in the city center and the holy shrine parking could be also ascribed to vehicular traffic, mainly by passenger buses. Supportively, researches argued that slow-moving vehicles made a major contribution in the PAHs emission in urban areas.

References

Aceves, M., Grimalt, J.O., 1993. Seasonally dependent size distributions of aliphatic and polycyclic aromatic hydrocarbons in urban aerosols from densely populated areas. Environmental Science & Technology 27, 2896-2908.

Aldabe, J., Elustondo, D., Santamaría, C., Lasheras, E., Pandolfi, M., Alastuey, A., Querol, X., Santamaría, J., 2011. Chemical characterisation and source apportionment of PM2. 5 and PM10 at rural, urban and traffic sites in Navarra (North of Spain). Atmospheric Research 102, 191-205.

Ali, M.U., Siyi, L., Yousaf, B., Abbas, Q., Hameed, R., Zheng, C., Kuang, X., Wong, M.H., 2020. Emission sources and full spectrum of health impacts of black carbon associated polycyclic aromatic hydrocarbons (PAHs) in urban environment: A review. Critical Reviews in Environmental Science and Technology, 1-40.

Alves, C., Vicente, A., Calvo, A., Baumgardner, D., Amato, F., Querol, X., Pio, C., Gustafsson, M., 2019. Physical and chemical properties of non-exhaust particles generated from wear between pavements and tyres. Atmospheric environment, 117252.

Azari, K.A., Arintono, S., 2012. Congestion pricing scheme in Mashhad, Iran: overview description, impacts and behavioural responsiveness. World Appl. Sci. J 20.

Azimi, A., Bakhtiari, A.R., Tauler, R., 2018. Chemometrics analysis of petroleum hydrocarbons sources in the street dust, runoff and sediment of urban rivers in Anzali port-South of Caspian Sea. Environmental Pollution 243, 374-382.

Bakhtiari, A.R., Zakaria, M.P., Yaziz, M.I., Lajis, M.N.H., Bi, X., 2009. Polycyclic aromatic hydrocarbons and n-alkanes in suspended particulate matter and sediments from the Langat River, Peninsular Malaysia. Environ. Asia 2, 1-10.

Bandowe, B.A.M., Nkansah, M.A., 2016. Occurrence, distribution and health risk from polycyclic aromatic compounds (PAHs, oxygenated-PAHs and azaarenes) in street dust from a major West African Metropolis. Science of The Total Environment 553, 439-449.

Belis, C., Offenthaler, I., Uhl, M., Nurmi-Legat, J., Bassan, R., Jakobi, G., Kirchner, M., Knoth, W., Kräuchi, N., Levy, W., 2009. A comparison of Alpine emissions to forest soil and spruce needle loads for persistent organic pollutants (POPs). Environmental pollution 157, 3185-3191.

Caricchia, A.M., Chiavarini, S., Pezza, M., 1999. Polycyclic aromatic hydrocarbons in the urban atmospheric particulate matter in the city of Naples (Italy). Atmospheric environment 33, 3731-3738.

Chung, M., Hu, R., Cheung, K., Wong, M.H., 2007. Pollutants in Hong Kong soils: polycyclic aromatic hydrocarbons. Chemosphere 67, 464-473.

Dong, T.T., Lee, B.-K., 2009. Characteristics, toxicity, and source apportionment of polycylic aromatic hydrocarbons (PAHs) in road dust of Ulsan, Korea. Chemosphere 74, 1245-1253.

EPA, U., 1991. Risk assessment guidance for superfund, Volume 1, Human health evaluation manual (Part B, Development of risk-based preliminary remediation goals). OSWER.

Fang, G.-C., Chang, C.-N., Wu, Y.-S., Fu, P.P.-C., Yang, I.-L., Chen, M.-H., 2004. Characterization, identification of ambient air and road dust polycyclic aromatic hydrocarbons in central Taiwan, Taichung. Science of The Total Environment 327, 135-146.

Franco, C.F.J., de Resende, M.F., de Almeida Furtado, L., Brasil, T.F., Eberlin, M.N., Netto, A.D.P., 2017. Polycyclic aromatic hydrocarbons (PAHs) in street dust of Rio de Janeiro and Niterói, Brazil: particle size distribution, sources and cancer risk assessment. Science of the total environment 599, 305-313.

Garcia, K.O., Teixeira, E.C., Agudelo-Castañeda, D.M., Braga, M., Alabarse, P.G., Wiegand, F., Kautzmann, R.M., Silva, L.F., 2014. Assessment of nitro-polycyclic aromatic hydrocarbons in PM1 near an area of heavy-duty traffic. Science of the total environment 479, 57-65.
Ghanavati, N., Nazarpour, A., Watts, M.J., 2019. Status, source, ecological and health risk assessment of toxic metals and polycyclic aromatic hydrocarbons (PAHs) in street dust of Abadan, Iran. Catena 177, 246-259.
Gope, M., Masto, R.E., Basu, A., Bhattacharyya, D., Saha, R., Hoque, R.R., Khillare, P., Balachandran, S., 2020. Elucidating the distribution and sources of street dust bound PAHs in Durgapur, India: a probabilistic health risk assessment study by Monte-Carlo simulation. Environmental Pollution, 115669.
Gope, M., Masto, R.E., George, J., Balachandran, S., 2018. Exposure and cancer risk assessment of polycyclic aromatic hydrocarbons (PAHs) in the street dust of Asansol city, India. Sustainable cities and society 38, 616-626.
Guo, H., Lee, S., Ho, K., Wang, X., Zou, S., 2003. Particle-associated polycyclic aromatic hydrocarbons in urban air of Hong Kong. Atmospheric Environment 37, 5307-5317.
Harrison, R.M., Smith, D., Luhana, L., 1996. Source apportionment of atmospheric polycyclic aromatic hydrocarbons collected from an urban location in Birmingham, UK. Environmental Science & Technology 30, 825-832.
Hassanien, M.A., Abdel-Latif, N.M., 2008. Polycyclic aromatic hydrocarbons in road dust over Greater Cairo, Egypt. Journal of Hazardous Materials 151, 247-254.
Huo, C.-Y., Sun, Y., Liu, L.-Y., Sverko, E., Li, Y.-F., Li, W.-L., Ma, W.-L., Zhang, Z.-F., Song, W.-W., 2019. Assessment of human indoor exposure to PAHs during the heating and non-heating season: Role of window films as passive air samplers. Science of The Total Environment 659, 293-301.
Hussain, K., Rahman, M., Prakash, A., Hoque, R.R., 2015. Street dust bound PAHs, carbon and heavy metals in Guwahati city–Seasonality, toxicity and sources. Sustainable cities and society 19, 17-25.
Jafarabadi, A.R., Bakhtiari, A.R., Aliabadian, M., Toosi, A.S., 2017. Spatial distribution and composition of aliphatic hydrocarbons, polycyclic aromatic hydrocarbons and hopanes in superficial sediments of the coral reefs of the Persian Gulf, Iran. Environmental Pollution 224, 195-223.
Javed, W., Iakovides, M., Garaga, R., Stephanou, E.G., Kota, S.H., Ying, Q., Wolfson, J.M., Koutrakis, P., Guo, B., 2019. Source apportionment of organic pollutants in fine and coarse atmospheric particles in Doha, Qatar. Journal of the Air & Waste Management Association 69, 1277-1292.
Jiang, Y., Hu, X., Yves, U.J., Zhan, H., Wu, Y., 2014. Status, source and health risk assessment of polycyclic aromatic hydrocarbons in street dust of an industrial city, NW China. Ecotoxicology and environmental safety 106, 11-18.
Keshavarzi, B., Abbasi H, S., Moore, F., Delshab, H., Soltani, N., 2020. Polycyclic aromatic hydrocarbons in street dust of Bushehr City, Iran: status, source, and human health risk assessment. Polycyclic Aromatic Compounds 40, 61-75.
Khalili, N.R., Scheff, P.A., Holsen, T.M., 1995. PAH source fingerprints for coke ovens, diesel and, gasoline engines, highway tunnels, and wood combustion emissions. Atmospheric Environment 29, 533-542.
Khpalwak, W., Jadoon, W.A., Abdel-Dayem, S.M., Sakugawa, H., 2019. Polycyclic aromatic hydrocarbons in urban road dust, Afghanistan: Implications for human health. Chemosphere 218, 517-526.
Kim, K.-H., Jahan, S.A., Kabir, E., Brown, R.J., 2013. A review of airborne polycyclic aromatic hydrocarbons (PAHs) and their human health effects. Environment international 60, 71-80.
Lang, Y.-H., Li, G.-L., Wang, X.-M., Peng, P., 2015. Combination of Unmix and PMF receptor model to apportion the potential sources and contributions of PAHs in wetland soils from Jiaozhou Bay, China. Marine pollution bulletin 90, 129-134.
Larsen, R.K., Baker, J.E., 2003. Source apportionment of polycyclic aromatic hydrocarbons in the urban atmosphere: a comparison of three methods. Environmental Science & Technology 37, 1873-1881.
Li, Y., Song, N., Yu, Y., Yang, Z., Shen, Z., 2017. Characteristics of PAHs in street dust of Beijing and the annual wash-off load using an improved load calculation method. Science of The Total Environment 581, 328-336.
Liao, C.-M., Chiang, K.-C., 2006. Probabilistic risk assessment for personal exposure to carcinogenic polycyclic aromatic hydrocarbons in Taiwanese temples. Chemosphere 63, 1610-1619.

Liu, J., Zhang, J., Zhan, C., Liu, H., Zhang, L., Hu, T., Xing, X., Qu, C., 2019. Polycyclic aromatic hydrocarbons (PAHs) in urban street dust of Huanggang, central China: Status, sources and human health risk assessment. Aerosol and Air Quality Research 19, 221-233.
Liu, M., Cheng, S., Ou, D., Hou, L., Gao, L., Wang, L., Xie, Y., Yang, Y., Xu, S., 2007. Characterization, identification of road dust PAHs in central Shanghai areas, China. Atmospheric Environment 41, 8785-8795.
Liu, Y., Chen, L., Huang, Q.-h., Li, W.-y., Tang, Y.-j., Zhao, J.-f., 2009. Source apportionment of polycyclic aromatic hydrocarbons (PAHs) in surface sediments of the Huangpu River, Shanghai, China. Science of The Total Environment 407, 2931-2938.
Lorenzi, D., Entwistle, J.A., Cave, M., Dean, J.R., 2011. Determination of polycyclic aromatic hydrocarbons in urban street dust: implications for human health. Chemosphere 83, 970-977.
Ma, Y., Liu, A., Egodawatta, P., McGree, J., Goonetilleke, A., 2017. Quantitative assessment of human health risk posed by polycyclic aromatic hydrocarbons in urban road dust. Science of The Total Environment 575, 895-904.
Majumdar, D., Rajaram, B., Meshram, S., Chalapati Rao, C., 2012. PAHs in road dust: ubiquity, fate, and summary of available data. Critical Reviews in Environmental Science and Technology 42, 1191-1232.
Malcolm, H., Dobson, S., 1994. The calculation of a Regulatory Assessment Level (RAL) for atmospheric PAHs based on relative potencies. first draft.
Maliszewska-Kordybach, B., 1996. Polycyclic aromatic hydrocarbons in agricultural soils in Poland: preliminary proposals for criteria to evaluate the level of soil contamination. Applied Geochemistry 11, 121-127.
Martuzevicius, D., Kliucininkas, L., Prasauskas, T., Krugly, E., Kauneliene, V., Strandberg, B., 2011. Resuspension of particulate matter and PAHs from street dust. Atmospheric environment 45, 310-317.
Moeinaddini, M., Sari, A.E., Bakhtiari, A.R., Chan, A.Y.-C., Taghavi, S.M., Connell, D., Hawker, D., 2014a. Sources and Health Risk of Organic Compounds in Respirable Particles in Tehran, Iran. Polycyclic Aromatic Compounds 34, 469-492.
Moeinaddini, M., Sari, A.E., Chan, A.Y.-C., Taghavi, S.M., Hawker, D., Connell, D., 2014b. Source apportionment of PAHs and n-alkanes in respirable particles in Tehran, Iran by wind sector and vertical profile. Environmental Science and Pollution Research 21, 7757-7772.
Mon, E.E., Phay, N., Agusa, T., Bach, L.T., Yeh, H.-M., Huang, C.-H., Nakata, H., 2020. Polycyclic Aromatic Hydrocarbons (PAHs) in Road Dust Collected from Myanmar, Japan, Taiwan, and Vietnam. Archives of environmental contamination and toxicology 78, 34-45.
Mostafa, A., Hegazi, A., El-Gayar, M.S., Andersson, J., 2009. Source characterization and the environmental impact of urban street dusts from Egypt based on hydrocarbon distributions. Fuel 88, 95-104.
Najmeddin, A., Keshavarzi, B., 2019. Health risk assessment and source apportionment of polycyclic aromatic hydrocarbons associated with PM 10 and road deposited dust in Ahvaz metropolis of Iran. Environmental geochemistry and health 41, 1267-1290.
Najmeddin, A., Moore, F., Keshavarzi, B., Sadegh, Z., 2018. Pollution, source apportionment and health risk of potentially toxic elements (PTEs) and polycyclic aromatic hydrocarbons (PAHs) in urban street dust of Mashhad, the second largest city of Iran. Journal of Geochemical Exploration 190, 154-169.
Nisbet, I.C., Lagoy, P.K., 1992. Toxic equivalency factors (TEFs) for polycyclic aromatic hydrocarbons (PAHs). Regulatory toxicology and pharmacology 16, 290-300.
Omar, N.Y.M., Abas, M.R.B., Ketuly, K.A., Tahir, N.M., 2002. Concentrations of PAHs in atmospheric particles (PM-10) and roadside soil particles collected in Kuala Lumpur, Malaysia. Atmospheric environment 36, 247-254.
Pant, P., Harrison, R.M., 2013. Estimation of the contribution of road traffic emissions to particulate matter concentrations from field measurements: a review. Atmospheric Environment 77, 78-97.
Park, S.S., Kim, Y.J., Kang, C.H., 2002. Atmospheric polycyclic aromatic hydrocarbons in Seoul, Korea. Atmospheric Environment 36, 2917-2924.
Ravindra, K., Bencs, L., Wauters, E., De Hoog, J., Deutsch, F., Roekens, E., Bleux, N., Berghmans, P., Van Grieken, R., 2006. Seasonal and site-specific variation in vapour and aerosol phase PAHs over

607 Flanders (Belgium) and their relation with anthropogenic activities. Atmospheric Environment 40, 771-
608 785.
609 Ravindra, K., Sokhi, R., Van Grieken, R., 2008. Atmospheric polycyclic aromatic hydrocarbons: source
610 attribution, emission factors and regulation. Atmospheric Environment 42, 2895-2921.
611 Simoneit, B.R., 1984. Organic matter of the troposphere—III. Characterization and sources of
612 petroleum and pyrogenic residues in aerosols over the western United States. Atmospheric Environment
613 (1967) 18, 51-67.
614 Škrbić, B., Đurišić-Mladenović, N., Živančev, J., Tadić, Đ., 2019. Seasonal occurrence and cancer risk
615 assessment of polycyclic aromatic hydrocarbons in street dust from the Novi Sad city, Serbia. Science
616 of The Total Environment 647, 191-203.
617 Soltani, N., Keshavarzi, B., Moore, F., Tavakol, T., Lahijanzadeh, A.R., Jaafarzadeh, N., Kermani, M.,
618 2015. Ecological and human health hazards of heavy metals and polycyclic aromatic hydrocarbons
619 (PAHs) in road dust of Isfahan metropolis, Iran. Science of The Total Environment 505, 712-723.
620 Song, Z., You, M., Duzgoren-Aydin, N.S., 2005. Characterization of particulate organics accumulated
621 on the ceiling of vehicular tunnels in Hong Kong and Guangzhou, China. Atmospheric Environment
622 39, 6398-6408.
623 Sulong, N.A., Latif, M.T., Sahani, M., Khan, M.F., Fadzil, M.F., Tahir, N.M., Mohamad, N., Sakai, N.,
624 Fujii, Y., Othman, M., 2019. Distribution, sources and potential health risks of polycyclic aromatic
625 hydrocarbons (PAHs) in PM2. 5 collected during different monsoon seasons and haze episode in Kuala
626 Lumpur. Chemosphere 219, 1-14.
627 Takada, H., Onda, T., Harada, M., Ogura, N., 1991. Distribution and sources of polycyclic aromatic
628 hydrocarbons (PAHs) in street dust from the Tokyo Metropolitan area. Science of The Total
629 Environment 107, 45-69.
630 Talebian, K., Riza, M., 2020. Mashhad, City of Light. Cities 101, 102674.
631 Teixeira, E.C., Agudelo-Castañeda, D.M., Mattiuzi, C.D.P., 2015. Contribution of polycyclic aromatic
632 hydrocarbon (PAH) sources to the urban environment: A comparison of receptor models. Science of
633 The Total Environment 538, 212-219.
634 Teixeira, E.C., Mattiuzi, C.D.P., Agudelo-Castañeda, D.M., de Oliveira Garcia, K., Wiegand, F., 2013.
635 Polycyclic aromatic hydrocarbons study in atmospheric fine and coarse particles using diagnostic ratios
636 and receptor model in urban/industrial region. Environmental Monitoring and Assessment 185, 9587-
637 9602.
638 Tobiszewski, M., Namieśnik, J., 2012. PAH diagnostic ratios for the identification of pollution emission
639 sources. Environmental Pollution 162, 110-119.
640 Wang, J., Zhang, X., Ling, W., Liu, R., Liu, J., Kang, F., Gao, Y., 2017. Contamination and health risk
641 assessment of PAHs in soils and crops in industrial areas of the Yangtze River Delta region, China.
642 Chemosphere 168, 976-987.
643 Wang, L., Wang, L., Tao, W., Smardon, R.C., Shi, X., Lu, X., 2016. Characteristics, sources, and health
644 risk of polycyclic aromatic hydrocarbons in urban surface dust: a case study of the city of Xi'an in
645 Northwest China. Environmental Science and Pollution Research 23, 13389-13402.
646 Wang, W., Huang, M.-j., Kang, Y., Wang, H.-s., Leung, A.O., Cheung, K.C., Wong, M.H., 2011a.
647 Polycyclic aromatic hydrocarbons (PAHs) in urban surface dust of Guangzhou, China: Status, sources
648 and human health risk assessment. Science of The Total Environment 409, 4519-4527.
649 Wang, W., Huang, M.J., Kang, Y., Wang, H.S., Leung, A.O., Cheung, K.C., Wong, M.H., 2011b.
650 Polycyclic aromatic hydrocarbons (PAHs) in urban surface dust of Guangzhou, China: Status, sources
651 and human health risk assessment. Sci Total Environ 409, 4519-4527.
652 Xia, F., Zhang, C., Qu, L., Song, Q., Ji, X., Mei, K., Dahlgren, R.A., Zhang, M., 2020. A comprehensive
653 analysis and source apportionment of metals in riverine sediments of a rural-urban watershed. Journal
654 of hazardous materials 381, 121230.
655 Xu, L., Shu, X., Hollert, H., 2016. Aggregate risk assessment of polycyclic aromatic hydrocarbons from
656 dust in an urban human settlement environment. Journal of Cleaner Production 133, 378-388.
657 Yadav, I.C., Devi, N.L., Li, J., Zhang, G., 2018. Polycyclic aromatic hydrocarbons in house dust and
658 surface soil in major urban regions of Nepal: Implication on source apportionment and toxicological
659 effect. Sci Total Environ 616-617, 223-235.
660 Yang, H.-H., Lee, W.-J., Chen, S.-J., Lai, S.-O., 1998. PAH emission from various industrial stacks.
661 Journal of hazardous materials 60, 159-174.

662 Yunker, M.B., Macdonald, R.W., Vingarzan, R., Mitchell, R.H., Goyette, D., Sylvestre, S., 2002. PAHs
663 in the Fraser River basin: a critical appraisal of PAH ratios as indicators of PAH source and
664 composition. Organic Geochemistry 33, 489-515.
665 Zakaria, M.P., Horinouchi, A., Tsutsumi, S., Takada, H., Tanabe, S., Ismail, A., 2000. Oil pollution in
666 the Straits of Malacca, Malaysia: Application of molecular markers for source identification.
667 Environmental Science & Technology 34, 1189-1196.
668 Zhang, Z.-H., Khlystov, A., Norford, L.K., Tan, Z.-K., Balasubramanian, R., 2017. Characterization of
669 traffic-related ambient fine particulate matter (PM2. 5) in an Asian city: Environmental and health
670 implications. Atmospheric Environment 161, 132-143.
671 Zhen, X.L., Liu, G., Li, J.H., Xu, H., Wu, D., 2020. PAHs in road dust of Nanjing Chemical Industry
672 Park, China: chemical composition, sources, and risk assessment. Journal of Environmental Science
673 and Health, Part A 55, 33-43.
674 Zheng, H., Yang, D., Hu, T., Li, Y., Zhu, G., Xing, X., Qi, S., 2017. Source apportionment of polycyclic
675 aromatic carbons (PAHs) in sediment core from Honghu Lake, central China: comparison study of three
676 receptor models. Environmental Science and Pollution Research 24, 25899-25911.

677

678